Structural and Multidisciplinary Optimization, 48(5), pp 893-907

Time-Dependent Reliability Analysis with Joint Upcrossing Rates

Zhen Hu and Xiaoping Du[*]

Department of Mechanical and Aerospace Engineering
Missouri University of Science and Technology
Rolla, Missouri 65409, U.S.A.

***Corresponding author**

Dr. Xiaoping Du

Department of Mechanical and Aerospace Engineering
Missouri University of Science and Technology
400 West 13th Street, Toomey Hall 290D,
Rolla, MO 65401, U.S.A.
Tel: 1-573-341-7249
Fax: 1-573-341-4607
E-mail: dux@mst.edu

Abstract

In time-dependent reliability analysis, an upcrossing is defined as the event when a limit-state function reaches its failure region from its safe region. Upcrossings are commonly assumed to be independent. The assumption may not be valid for some applications and may result in large errors. In this work, we develop a more accurate method that relaxes the assumption by using joint upcrossing rates. The method extends the existing joint upcrossing rate method to general limit-state functions with both random variables and stochastic processes. The First Order Reliability Method (FORM) is employed to derive the single upcrossing rate and joint upcrossing rate. With both rates, the probability density of the first time to failure can be solved numerically. Then the probability density leads to an easy evaluation of the time-dependent probability of failure. The proposed method is applied to the reliability analysis of a beam and a mechanism, and the results demonstrate a significant improvement in accuracy.

Keywords: Time-dependent reliability, stochastic processes, first passage, autocorrelation

1. Introduction

Reliability is the probability that a product performs its intended function over a specified period of time and under specified service conditions [1]. Depending on whether the performance of the product is time-dependent or not, reliability can be classified into two types: *time-variant* (*time-dependent*) *reliability* and *time-invariant reliability*.

For a time-invariant performance, its reliability and probability of failure remain constant over time. The time-invariant probability of failure is defined by

$$p_f = \Pr\left\{D = g(\mathbf{X}) > e\right\} \tag{1}$$

where $\mathbf{X} = (X_1, X_2, \cdots X_n)$ is a random vector, $g(\cdot)$ is a time-invariant performance function or limit-state function, D is a performance variable, e is a limit state, and $\Pr\{\cdot\}$ stands for a probability. Many reliability methods are available for calculating the time-invariant reliability, including the First Order Second Moment Method (FOSM), FORM, and Second Order Reliability Method (SORM) [2-8].

On the other hand, limit-state functions may vary over time. For instance, over the service life of the Thermal Barrier Coating (TBC) of aircraft engines, the stresses and strains of the TBC are time dependent [9]. Many mechanisms also experience time varying random motion errors due to random dimensions (tolerances), clearances, and deformations of structural components [10-14]. In the systems of wind turbines, hydrokinetic turbines, and aircraft turbine engines, the turbine blade loading always varies over time. Likewise, the wave loading acting on offshore structures fluctuates randomly with time [15-17]. Almost all dynamic systems involve time-dependent parameters [18-20]. For all the above problems, reliability is a function of time and typically deteriorates with time.

Therefore, a general limit-state function is a function of time t. In addition to random variables $\mathbf{X} = (X_1, X_2, \cdots X_n)$, stochastic processes $\mathbf{Y}(t) = (Y_1(t), Y_2(t), \cdots Y_m(t))$ may also appear in the limit-state function. A stochastic process can be considered as a random variable that varies over time. Hence a general time-dependent limit-state function is given by

$$D(t) = g(\mathbf{X}, \mathbf{Y}(t), t) \tag{2}$$

If we want to know the likelihood of failure at a particular instant of time t, we can still use the time-invariant probability of failure because t is fixed at the instant. Using Eq. (1), we obtain the instantaneous probability of failure

$$p_f(t) = \Pr\{g(\mathbf{X}, \mathbf{Y}(t), t) > e(t)\} \tag{3}$$

The aforementioned methods, such as FOSM, FORM, or SORM, are ready to calculate $p_f(t)$.

For time-dependent problems, we are more concerned with the time-dependent probability of failure because it provides us with the likelihood of a product performing its intended function over its service time, or a system fulfilling its task during its mission time. The time-dependent probability of failure over a time interval $[t_0, t_s]$ is defined by

$$p_f(t_0, t_s) = \Pr\{g(\mathbf{X}, \mathbf{Y}(\tau), \tau) > e(\tau),\ \exists\, \tau \in [t_0, t_s]\} \tag{4}$$

where t_0 is the initial time when the product is put into operation, and t_s is the endpoint of the time interval, such as the service time of the product.

Let the first time to failure (FTTF) be T_1, which is the time that $g(\cdot)$ reaches its limit state for the first time. T_1 is also the working time before failure and is obviously a random variable. $p_f(t_0, t_s)$ can also be given by

$$p_f(t_0, t_s) = F_{T_1}(t_s) = \Pr\{T_1 < t_s\} \tag{5}$$

where $F_{T_1}(\cdot)$ is the cumulative distribution function (CDF) of the FTTF.

Time-dependent reliability methodologies are classified into two categories. The first includes the extreme-value methods, which use the time-invariant reliability analysis methods (FOSM, FORM, SORM, etc.) if one can obtain the distribution of the extreme value of $g(\mathbf{X}, \mathbf{Y}(\tau)) - e(\tau)$ over $[t_0, t_s]$ [21-23]. The reason is that the failure event $\{g(\mathbf{X}, \mathbf{Y}(\tau), \tau) > e(\tau),\ \exists\, \tau \in [t_0, t_s]\}$ is equivalent to the event

$\left\{\max_{\tau}\left[g(\mathbf{X},\mathbf{Y}(\tau))-e(\tau)\right]>0,\ \exists\,\tau\in[t_0,t_s]\right\}$. However, it is difficult to obtain the distribution of the extreme value. Therefore, in most cases, the methods in the second category are used.

The second category includes the first-passage methods because they directly use the first-passage time or the first time to failure (FTTF) T_1 in Eq. (5). The failure event $\{g(\mathbf{X},\mathbf{Y}(\tau),\tau)>e(\tau),\ \exists\,\tau\in[t_0,t_s]\}$ is equivalent to the event that at least a failure occurs over $[t_0,t_s]$ or equivalent to the event of $t_0\le T_1\le t_s$. The most commonly used method is the Rice's formula [24], which is based on the concept of upcrossing.

Define $N(t_0,t_s)$ as the number of upcrossings that $g(\cdot)$ reaches the limit state e from the safe region $g(\cdot)<0$ over the time period $[t_0,t_s]$. The basic probability theory shows that $N(t_0,t_s)$ follows a binomial distribution. When the probability of upcrossing is very small, it is equal to the mean number of upcrossings per unit time (the upcrossing rate). Because the binomial distribution converges to the Poisson distribution when the time period is sufficiently long or the dependence between crossings is negligible, the upcrossings are assumed to be statistically independent [25]. With this assumption, the upcrossing rate becomes the first-time crossing rate or the failure rate. Then the probability of failure can be estimated from the upcrossing rate.

Since the development of the Rice's formula, many improvements have been made [26-38]. For example, an analytical outcrossing rate [29] has been derived for Gaussian stationary processes. An analytical outcrossing rate has also been given for general Gaussian stochastic processes [30, 31] and has been applied to mechanism analysis [32]. If upcrossing events are rare over the considered time period [32], the Poisson assumption-based approaches [26-38] have shown good accuracy.

When upcrossings are strongly dependent, however, the above approaches may leads to large errors. In this case, the memory of failure should be considered to guarantee that the obtained first passage failure is indeed the first. Even though the Markov process methods have a property of memory, such memory is weak and is only valid for Markov or similar processes [39, 40]. Vanmarcke [41] and Preumont [42] have made some empirical modifications to the Poisson assumption-based formulas. These modifications are good for Gaussian processes.

A promising way to improve accuracy is to relax the independent assumption for upcrossing events. In other words, we may consider the dependence between two or more instants of time [43, 44], instead of considering a single upcrossing at one instant. The accuracy improvement has been shown in [44] for a Gaussian process in vibration problems.

Inspired by the work in [44], we develop a time-dependent reliability analysis method with joint upcrossing rates, which extends the method in [44] to more general limit-state functions that involve time, random variables, and stochastic processes. Because the method combines the joint upcrossing rates (JUR) and First Oder Reliability Method (FORM), we call it JUR/FORM.

In section 2, we review the commonly used time-dependent reliability analysis methods upon which JUR/FORM is built. We then discuss JUR/FORM in Section 3 followed by two case studies in Section 4. Conclusions are made in Section 5.

2. Review of time-dependent reliability analysis methods

In this section, we review the integration of the Poisson assumption based method with the First Order Reliability Method (FORM). By this method, $p_f(t_0, t_s)$ is calculated by [32, 44]

$$p_f(t_0, t_s) = 1 - [1 - p_f(t_0)]\exp\left\{-\int_{t_0}^{t_s} v^+(t)dt\right\} \tag{6}$$

where $p_f(t_0)$ is the instantaneous probability of failure at the initial time point t_0, and $v^+(t)$ is the upcrossing rate at t.

$p_f(t_0)$ can be calculated by any time-invariant reliability methods, such as FOSM, FORM, and SORM. If we know $v^+(t)$, then we can calculate $p_f(t_0, t_s)$ by integrating $v^+(t)$ over $[t_0, t_s]$ as indicated in Eq. (6).

For a general limit-state function $D(t) = g(\mathbf{X}, \mathbf{Y}(t), t)$, at a given instant t, the stochastic proceses $\mathbf{Y}(t)$ become random variables. If we use FORM, we first transform random variables $(\mathbf{X}, \mathbf{Y}(t))$ into standard normal variables $\mathbf{U}(t) = (\mathbf{U}_{\mathbf{X}}, \mathbf{U}_{\mathbf{Y}}(t))$ [2-6, 32]. Then we search for the Most Probable Point (MPP) $\tilde{\mathbf{U}}(t) = (\tilde{\mathbf{U}}_{\mathbf{X}}, \tilde{\mathbf{U}}_{\mathbf{Y}}(t))$. The MPP is a point at the limit sate, and at this point the limit-state function has its highest probability density. After the limit-state function is linearized at the MPP, the failure event $g(\mathbf{X}, \mathbf{Y}(t), t) > e(t)$ is equivalent to the event given by [1].

$$W(\mathbf{U}(t), t) = \boldsymbol{\alpha}(t)\mathbf{U}(t)^T > \beta(t) \tag{7}$$

where

$$\boldsymbol{\alpha}(t) = \left. \frac{\partial \mathbf{g}(T[\mathbf{U}(t)], t)}{\partial \mathbf{U}(t)} \right|_{\tilde{\mathbf{U}}(t)} \Bigg/ \left\| \left. \frac{\partial \mathbf{g}(T[\mathbf{U}(t)], t)}{\partial \mathbf{U}(t)} \right|_{\tilde{\mathbf{U}}(t)} \right\| \\ = \nabla \mathbf{g}(T[\tilde{\mathbf{U}}(t)], t) \Big/ \left\| \nabla \mathbf{g}(T[\tilde{\mathbf{U}}(t)], t) \right\| \tag{8}$$

$\beta(t)$ is the reliability index, which is the length of $\tilde{\mathbf{U}}(t)$. $T(\cdot)$ is the operator of transforming non-Gaussian random variables $(\mathbf{X}, \mathbf{Y}(t))$ into Gaussian random variables $\mathbf{U}(t)$. $\|\cdot\|$ stands for the magnitude of a vector.

Then the upcrossing rate $v^+(t)$ is [45]

$$v^+(t) = \|\dot{\boldsymbol{\alpha}}(t)\| \phi(\beta(t)) \Psi\left(\dot{\beta}(t) / \|\dot{\boldsymbol{\alpha}}(t)\|\right) \tag{9}$$

where $\dot{\boldsymbol{\alpha}}(t)$ and $\dot{\beta}(t)$ are the derivatives of $\boldsymbol{\alpha}(t)$ and $\beta(t)$, respectively, with respect to time *t*, and $\Psi(\cdot)$ is a function defined by

$$\Psi(x) = \phi(x) - x\Phi(-x) \tag{10}$$

in which $\phi(x)$ and $\Phi(-x)$ stand for the probability density function (PDF) and cumulative density function (CDF) of the standard normal random variable, respectively.

As mentioned previously, the above method may produce large errors if upcrossings are strongly dependent. Next we use the joint upcrossing rate to improve the accuracy of time-dependent reliability analysis.

3. Time-dependent reliability analysis with joint upcrossing rates and FORM

In this section, we first provide the equations given in [44] for a Gaussian stochastic process. Based on these equations and FORM, we then derive complete equations in the subsequent subsections.

3.1. Time-dependent reliability analysis with joint upcrossing rates

We now summarize the methodology in [44] where the joint upcrossing rates are used. Based on the methodologies, necessary equations are developed in Secs. 3.2 and 3.3.

For a general stochastic process $Q(t)$, suppose its failure event is defined by $\{Q(t) > e(t)\}$. $p_f(t_0, t) = \Pr\{Q(\tau) > e(\tau),\ \exists\, \tau \in [t_0, t_s]\}$ is then given by

$$p_f(t_0, t_s) = \Pr\{Q(t_0) > e(t_0)\} + \Pr\{Q(t_0) < e(t_0)\}\Pr\{Q(\tau) > e(\tau),\ \exists\, \tau \in [t_0, t_s]\} \tag{11}$$

or

$$p_f(t_0, t_s) = \Pr\{Q(t_0) > e(t_0)\} + \Pr\{Q(t_0) < e(t_0)\}\int_{t_0}^{t_s} f_{T_1}(t)\,dt \tag{12}$$

where $f_{T_1}(t)$ is the probability density function (PDF) of the first time to failure (FTTF). The first term in the above equation is the probability of failure at the initial time, and the second term is the probability of failure over $[t_0, t_s]$ and no failure occurs at t_0.

The upcrossing rate $v^+(t)$ is the probability that an upcrossing occurs at time t per unit of time. It is equal to the summation of two probabilities. The first probability is the PDF $f_{T_1}(t)$, which is the upcrossing rate occurring for the first time at t. The second probability is the probability rate that the upcrossing occurred at time t given that the first-time upcrossing occurs at time τ prior to t. Thus [44]

$$v^+(t) = f_{T_1}(t) + \int_{t_0}^{t} v^+(t|\tau) f_{T_1}(\tau)\,d\tau \tag{13}$$

According to the characteristics of conditional probability for two events A and B, we have $P(\mathrm{A}|\mathrm{B}) = P(\mathrm{A},\mathrm{B})/P(\mathrm{B})$. Thus, the conditional probability $v^+(t|\tau)$ is equal to $v^{++}(t,\tau)/v^+(t)$, and Eq. (13) is rewritten as

$$v^+(t) = f_{T_1}(t) + \int_{t_0}^{t} v^{++}(t,\tau) f_{T_1}(\tau) / v^+(\tau) d\tau \tag{14}$$

where $v^{++}(t,\tau)$ is the second order upcrossing rate or the joint outcrossing rate at t and τ. It indicates the joint probability that there are outcrossings at both t and τ.

After solving for $f_{T_1}(\tau)$ numerically using Eq. (14), we can obtain $p_f(t_0, t_s)$ with Eq. (12).

The above methodology is applicable for a single stochastic process. We now extend it to a general limit-state function $D(t) = g(\mathbf{X}, \mathbf{Y}(t), t)$. As $D(t)$ can be converted into a Gaussian process at the MPP, the extension is possible. Since both of the single and joint upcrossing rates are needed, we first derive equations for the two rates by using FORM and Rice's formula. We then discuss how to obtain the time-dependent probability of failure based on these rates.

3.2. Single upcrossing rate $v^+(t)$

Recall that after the MPP is found, the general limit-state function $g(\mathbf{X}, \mathbf{Y}(t), t)$ becomes $W(\mathbf{U}(t), t)$, and the failure event is $W(\mathbf{U}(t), t) = \boldsymbol{\alpha}(t)\mathbf{U}(t)^T > \beta(t)$. According to the Rice's formula [24, 46], the single upcrossing rate $v^+(t)$ is given by

$$v^+(t) = \omega(t)\phi(\beta(t))\Psi\left(\dot{\beta}(t)/\omega(t)\right) \tag{15}$$

where $\omega(t)$ is the standard deviation of $\dot{W}(t)$, which is the time derivative process of $W(t)$. $\omega^2(t)$ is given in terms of the correlation function $\rho(t_1, t_2)$ of $W(t)$ as follows:

$$\omega^2(t) = \partial^2 \rho(t_1, t_2) / (\partial t_1 \partial t_2)\Big|_{t_1 = t_2 = t} \tag{16}$$

We use the finite difference method to estimate $\dot{\beta}(t)$. This means that we need to perform the MPP search twice. Ref. [45] also uses the finite difference method but introduces additional random variables for the second MPP search. As will been seen, the method presented here does not introduce any extra random variables.

As mentioned above, $W(t) = \boldsymbol{\alpha}(t)\mathbf{U}(t)^T$, and from Eq. (8), we have $\|\boldsymbol{\alpha}(t)\| = 1$. $W(t)$ is therefore a standard normal stochastic process, and its coefficient of correlation is given by

$$\rho(t_1, t_2) = \boldsymbol{\alpha}(t_1)\mathbf{C}(t_1, t_2)\boldsymbol{\alpha}(t_2)^T \tag{17}$$

where $\mathbf{C}(t_1, t_2)$ is the covariance matrix of $\mathbf{U}(t_1)$ and $\mathbf{U}(t_2)$.

Since $\mathbf{U}(t) = (\mathbf{U_X}, \mathbf{U_Y}(t))$ is a vector of standard normal random variables and stochastic processes, $\mathbf{C}(t_1, t_2)$ is given by:

$$\mathbf{C}(t_1, t_2) = \begin{bmatrix} \mathbf{I}_{n\times n} & 0 \\ 0 & \mathbf{C}^Y(t_1, t_2) \end{bmatrix} \tag{18}$$

where $\mathbf{I}_{n\times n}$ is an $n \times n$ identity matrix, which is the covariance matrix of the normalized random variables $\mathbf{U_X}$ from $\mathbf{X}$. The covariance matrix of the normalized stochastic processes $\mathbf{U_Y}(t)$ from $\mathbf{Y}(t)$ is given in terms of its correlation coefficients as

$$\mathbf{C}^Y(t_1, t_2) = \begin{bmatrix} C^{Y_1}(t_1,t_2) & 0 & \cdots & 0 \\ 0 & \ddots & \cdots & 0 \\ \vdots & \vdots & \ddots & \vdots \\ 0 & 0 & \cdots & C^{Y_m}(t_1,t_2) \end{bmatrix} = \begin{bmatrix} \rho^{Y_1} & 0 & \cdots & 0 \\ 0 & \ddots & \cdots & 0 \\ \vdots & \vdots & \ddots & \vdots \\ 0 & 0 & \cdots & \rho^{Y_m} \end{bmatrix} \tag{19}$$

where $C(\cdot,\cdot)$ standard for the covariance, $C^{Y_i}(t_1,t_2)$ is the covariance of the normalized stochastic process $U_{Y_i}(t)$ at time instants t_1 and t_2. ρ^{Y_i} is the corresponding correlation function of the normalized stochastic process $U_{Y_i}(t)$ at these two time instants and is given by

$$\rho^{Y_i} = \rho^{Y_i}(t_1,t_2) \tag{20}$$

Substituting Eq. (17) into Eq. (16) yields

$$\begin{aligned}\omega^2(t) &= \partial^2 \rho(t_1, t_2) / (\partial t_1 \partial t_2)\Big|_{t_1=t_2=t} \\ &= \dot{\boldsymbol{\alpha}}(t)\dot{\mathbf{C}}_2(t,t)\boldsymbol{\alpha}(t)^T + \dot{\boldsymbol{\alpha}}(t)\mathbf{C}(t,t)\dot{\boldsymbol{\alpha}}(t)^T \\ &\quad + \boldsymbol{\alpha}(t)\ddot{\mathbf{C}}_{12}(t,t)\boldsymbol{\alpha}(t)^T + \boldsymbol{\alpha}(t)\dot{\mathbf{C}}_1(t,t)\dot{\boldsymbol{\alpha}}(t)^T\end{aligned} \tag{21}$$

Since we perform the MPP search at two instants and Eq. (21) also needs two instants (t, t), we now derive equations for two general instants t_1 and t_2. For time derivatives, such as $\dot{\beta}(t)$, we let $t_1 = t_1$, $t_2 = t_1 + \Delta t$, where Δt is a small step size.

Differentiating Eq. (18), we obtain

$$\dot{\mathbf{C}}_1(t_1, t_2) = \partial \mathbf{C}(t_1, t_2) / \partial t_1 = \begin{bmatrix} \mathbf{0} & 0 \\ 0 & \dot{\mathbf{C}}_1^Y(t_1, t_2) \end{bmatrix} \tag{22}$$

$$\dot{\mathbf{C}}_2(t_1, t_2) = \partial \mathbf{C}(t_1, t_2) / \partial t_2 = \begin{bmatrix} \mathbf{0} & 0 \\ 0 & \dot{\mathbf{C}}_2^Y(t_1, t_2) \end{bmatrix} \tag{23}$$

and

$$\ddot{\mathbf{C}}_{12}(t_1, t_2) = \begin{pmatrix} \mathbf{0} & 0 \\ 0 & \ddot{\mathbf{C}}_{12}^Y(t_1, t_2) \end{pmatrix} \tag{24}$$

$\dot{\mathbf{C}}_1^Y(t_1, t_2)$, $\dot{\mathbf{C}}_2^Y(t_1, t_2)$, and $\ddot{\mathbf{C}}_{12}^Y(t_1, t_2)$ are given by

$$\dot{C}_1^{Y_i}(t_1, t_2) = \partial \rho^{Y_i}(t_1, t_2) / \partial t_1, \;\; i = 1, 2, \cdots, m \tag{25}$$

$$\dot{C}_2^{Y_i}(t_1, t_2) = \partial \rho^{Y_i}(t_1, t_2) / \partial t_2, \;\; i = 1, 2, \cdots, m \tag{26}$$

and

$$\ddot{C}_{12}^{Y_i}(t_1, t_2) = \partial^2 \rho^{Y_i}(t_1, t_2) / (\partial t_1 \partial t_2), \;\; i = 1, 2, \cdots, m \tag{27}$$

Specially, for a pair of the same time instant (t, t), we have

$$\rho^{Y_i}(t, t) = 1 \tag{28}$$

$$\mathbf{C}(t, t) = \mathbf{I}_{n \times m} \tag{29}$$

$$\partial \rho^{Y_i}(t,t) / \partial t_1 = C\left(\dot{W}(t), W(t)\right) = 0 \quad (30)$$

$$\dot{\mathbf{C}}_1(t,t) = \mathbf{O}_{n\times m} \quad (31)$$

$$\partial \rho^{Y_i}(t,t) / \partial t_2 = C\left(W(t), \dot{W}(t)\right) = 0 \quad (32)$$

and

$$\dot{\mathbf{C}}_2(t,t) = \mathbf{O}_{n\times m} \quad (33)$$

Therefore, Eq. (21) is rewritten as

$$\omega(t)^2 = \dot{\boldsymbol{\alpha}}(t)\dot{\boldsymbol{\alpha}}(t)^T + \boldsymbol{\alpha}(t)\ddot{\mathbf{C}}_{12}(t,t)\boldsymbol{\alpha}(t)^T \quad (34)$$

where $\ddot{\mathbf{C}}_{12}(t,t)$ is computed by substituting (t_1, t_2) with (t,t) in Eq. (24), $\dot{\boldsymbol{\alpha}}(t)$ and $\dot{\beta}(t)$ are calculated by

$$\dot{\boldsymbol{\alpha}}(t) = (\boldsymbol{\alpha}(t+\Delta t) - \boldsymbol{\alpha}(t)) / \Delta t \quad (35)$$

and

$$\dot{\beta}(t) = (\beta(t+\Delta t) - \beta(t)) / \Delta t \quad (36)$$

We have obtained all the equations for the single upcrossing rate $v^+(t)$ in Eq. (15).

3.3. Joint upcrossing rate $v^{++}(t_1, t_2)$

Now we derive the joint upcrossing rate $v^{++}(t_1, t_2)$ between two arbitrary time instants t_1 and t_2. The joint upcrossing rate $v^{++}(t_1, t_2)$, which indicates the joint probability that outcrossing events occur at both t_1 and t_2, is defined by the Rice's formula as follows [24, 46] :

$$v^{++}(t_1, t_2) = \int_{\dot{\beta}_1}^{\infty}\int_{\dot{\beta}_2}^{\infty} f_{\dot{\mathbf{W}}\mathbf{W}}\left(\mathbf{Z}, \boldsymbol{\beta}\right)(z_1 - \dot{\beta}_1)(z_2 - \dot{\beta}_2)dz_1 dz_2 \quad (37)$$

where $f_{\dot{\mathbf{W}}\mathbf{W}}(\dot{\mathbf{W}},\mathbf{W})$ is the joint normal density function of $\dot{\mathbf{W}}=(\dot{W}(t_1),\dot{W}(t_2))$, and $\mathbf{W}=(W(t_1),W(t_2))$, $\boldsymbol{\beta}=(\beta_1,\beta_2)$, $\beta_1=\beta(t_1)$, and $\beta_2=\beta(t_2)$. The covariance matrix of $\dot{\mathbf{W}}$ and $\mathbf{W}$ is given by [44]

$$\mathbf{c}=\begin{bmatrix}\mathbf{c}_{\dot{\mathbf{W}}\dot{\mathbf{W}}} & \mathbf{c}_{\dot{\mathbf{W}}\mathbf{W}}\\ \mathbf{c}_{\mathbf{W}\dot{\mathbf{W}}} & \mathbf{c}_{\mathbf{W}\mathbf{W}}\end{bmatrix}=\begin{bmatrix}\omega^2(t_1) & \rho_{12} & 0 & \rho_1\\ \rho_{21} & \omega^2(t_2) & \rho_2 & 0\\ 0 & \rho_2 & 1 & \rho\\ \rho_1 & 0 & \rho & 1\end{bmatrix} \tag{38}$$

in which

$$\rho=\rho(t_1,t_2) \tag{39}$$

$$\rho_1=\partial\rho(t_1,t_2)/\partial t_1 \tag{40}$$

$$\rho_2=\partial\rho(t_1,t_2)/\partial t_2 \tag{41}$$

$$\rho_{12}=\partial^2\rho(t_1,t_2)/(\partial t_1\partial t_2) \tag{42}$$

and

$$\rho_{21}=\partial^2\rho(t_1,t_2)/(\partial t_2\partial t_1) \tag{43}$$

Substituting Eq. (17) into Eqs. (40)-(43) yields

$$\rho_1=\dot{\boldsymbol{\alpha}}(t_1)\mathbf{C}(t_1,t_2)\boldsymbol{\alpha}(t_2)^T+\boldsymbol{\alpha}(t_1)\dot{\mathbf{C}}_1(t_1,t_2)\boldsymbol{\alpha}(t_2)^T \tag{44}$$

$$\rho_2=\boldsymbol{\alpha}(t_1)\mathbf{C}(t_1,t_2)\dot{\boldsymbol{\alpha}}(t_2)^T+\boldsymbol{\alpha}(t_1)\dot{\mathbf{C}}_2(t_1,t_2)\boldsymbol{\alpha}(t_2)^T \tag{45}$$

$$\begin{aligned}\rho_{12}&=\dot{\boldsymbol{\alpha}}(t_1)\dot{\mathbf{C}}_2(t_1,t_2)\boldsymbol{\alpha}(t_2)^T+\dot{\boldsymbol{\alpha}}(t_1)\mathbf{C}(t_1,t_2)\dot{\boldsymbol{\alpha}}(t_2)^T\\&+\boldsymbol{\alpha}(t_1)\ddot{\mathbf{C}}_{12}(t_1,t_2)\boldsymbol{\alpha}(t_2)^T+\boldsymbol{\alpha}(t_1)\dot{\mathbf{C}}_1(t_1,t_2)\dot{\boldsymbol{\alpha}}(t_2)^T\end{aligned} \tag{46}$$

and

$$\begin{aligned}\rho_{21}&=\dot{\boldsymbol{\alpha}}(t_1)\mathbf{C}(t_1,t_2)\dot{\boldsymbol{\alpha}}(t_2)^T+\boldsymbol{\alpha}(t_1)\dot{\mathbf{C}}_1(t_1,t_2)\dot{\boldsymbol{\alpha}}(t_2)^T\\&+\boldsymbol{\alpha}(t_1)\ddot{\mathbf{C}}_{21}(t_1,t_2)\boldsymbol{\alpha}(t_2)^T+\dot{\boldsymbol{\alpha}}(t_1)\dot{\mathbf{C}}_2(t_1,t_2)\boldsymbol{\alpha}(t_2)^T\end{aligned} \tag{47}$$

in which

$$\ddot{\mathbf{C}}_{21}(t_1,t_2)=\begin{pmatrix}\mathbf{0} & 0\\ 0 & \ddot{\mathbf{C}}_{21}^{Y}(t_1,t_2)\end{pmatrix} \tag{48}$$

and

$$\ddot{C}_{21}^{Y_i}(t_1,t_2)=\partial^2\rho^{Y_i}(t_1,t_2)/(\partial t_1\partial t_2),\ \ i=1,2,\cdots,m \tag{49}$$

$\mathbf{C}(t_1,t_2)$, $\dot{\mathbf{C}}_1(t_1,t_2)$, $\dot{\mathbf{C}}_2(t_1,t_2)$, and $\ddot{\mathbf{C}}_{12}(t_1,t_2)$ in Eqs. (44)-(47) are computed using Eqs. (18), and (22) through (24).

With the above equations derived, we can now use the equations in [44] directly to calculate $v^{++}(t_1,t_2)$. The equations are summarized blow.

$$\begin{aligned}&v^{++}(t_1,t_2)=\lambda_1\lambda_2 f_{\mathbf{W}}(\boldsymbol{\beta})\Psi\left((\dot{\beta}_1-\mu_1)/\lambda_1\right)\Psi\left((\dot{\beta}_2-\mu_2)/\lambda_2\right)\\&+\lambda_1\lambda_2 f_{\mathbf{W}}(\boldsymbol{\beta})\kappa\Phi\left((\mu_1-\dot{\beta}_1)/\lambda_1\right)\Phi\left((\mu_2-\dot{\beta}_2)/\lambda_2\right)\\&+\lambda_1^2\lambda_2^2 f_{\mathbf{W}}(\boldsymbol{\beta})\int_0^{\kappa}(\kappa-K)\,f_{\dot{\mathbf{W}}|\mathbf{W}}\left(\dot{\boldsymbol{\beta}}\,|\,\boldsymbol{\beta};K\right)dK\end{aligned} \tag{50}$$

in which

$$f_{\mathbf{W}}(\boldsymbol{\beta})=(\exp((\beta_1^2-2\rho\beta_1\beta_2+\beta_2^2)/(2-2\rho^2)))/(2\pi\sqrt{1-\rho^2}) \tag{51}$$

μ_1 and μ_2, λ_1 and λ_2, κ are the mean values, standard deviations, and correlation coefficient of $\dot{W}(t_1)\big|\boldsymbol{\beta}$ and $\dot{W}(t_2)\big|\boldsymbol{\beta}$, respectively. They are calculated by substituting the covariance matrix in Eq. (38) into the following equations

$$\boldsymbol{\mu}=\begin{bmatrix}\mu_1\\ \mu_2\end{bmatrix}=\mathbf{c}_{\dot{\mathbf{W}}\mathbf{W}}\mathbf{c}_{\mathbf{W}\mathbf{W}}^{-1}\boldsymbol{\beta}=\begin{bmatrix}(\beta_2-\rho\beta_1)\rho_1\\ (\beta_1-\rho\beta_2)\rho_2\end{bmatrix}/(1-\rho^2) \tag{52}$$

$$\sum=\mathbf{c}_{\dot{\mathbf{W}}|\mathbf{W}}=\mathbf{c}_{\dot{\mathbf{W}}\dot{\mathbf{W}}}-\mathbf{c}_{\dot{\mathbf{W}}\mathbf{W}}\mathbf{c}_{\mathbf{W}\mathbf{W}}^{-1}\mathbf{c}_{\mathbf{W}\dot{\mathbf{W}}}=\begin{bmatrix}\lambda_1^2 & \kappa\lambda_1\lambda_2\\ \kappa\lambda_1\lambda_2 & \lambda_2^2\end{bmatrix} \tag{53}$$

After the derivation of $v^{+}(t)$ and $v^{++}(t_1, t_2)$, $p_f(t_0, t_s)$ is computed with Eqs. (12), (14), (15), and (50).

3.4. Numerical implementation

There are many equations involved in JUR/FORM. In this section, we summarize its numerical implementation. From Eq. (11) and (12), we know that to obtain $p_f(t_0, t_s)$, we need to integrate the PDF $f_{T_1}(t)$ over $[t_0, t_s]$ numerically. At each of the integration point between t_0 and t_s, the integral equation in Eq. (14) should be solved. To maintain good efficiency, we propose the following numerical procedure.

We start to evaluate the PDF at the last instant t_s. To do so, we discretize the time interval $[t_0, t_s]$ into $p+1$ instants t_i $(i = 0, 1, 2, \cdots, p)$, at each of which the integral equation in Eq. (14) for $f_{T_1}(t_s)$ will be solved. We will then obtain the PDFs at all these instants. Thus the total number of the MPP will be $2p$. This procedure is summarized below, and the associated flowchart is given in Fig. 1.

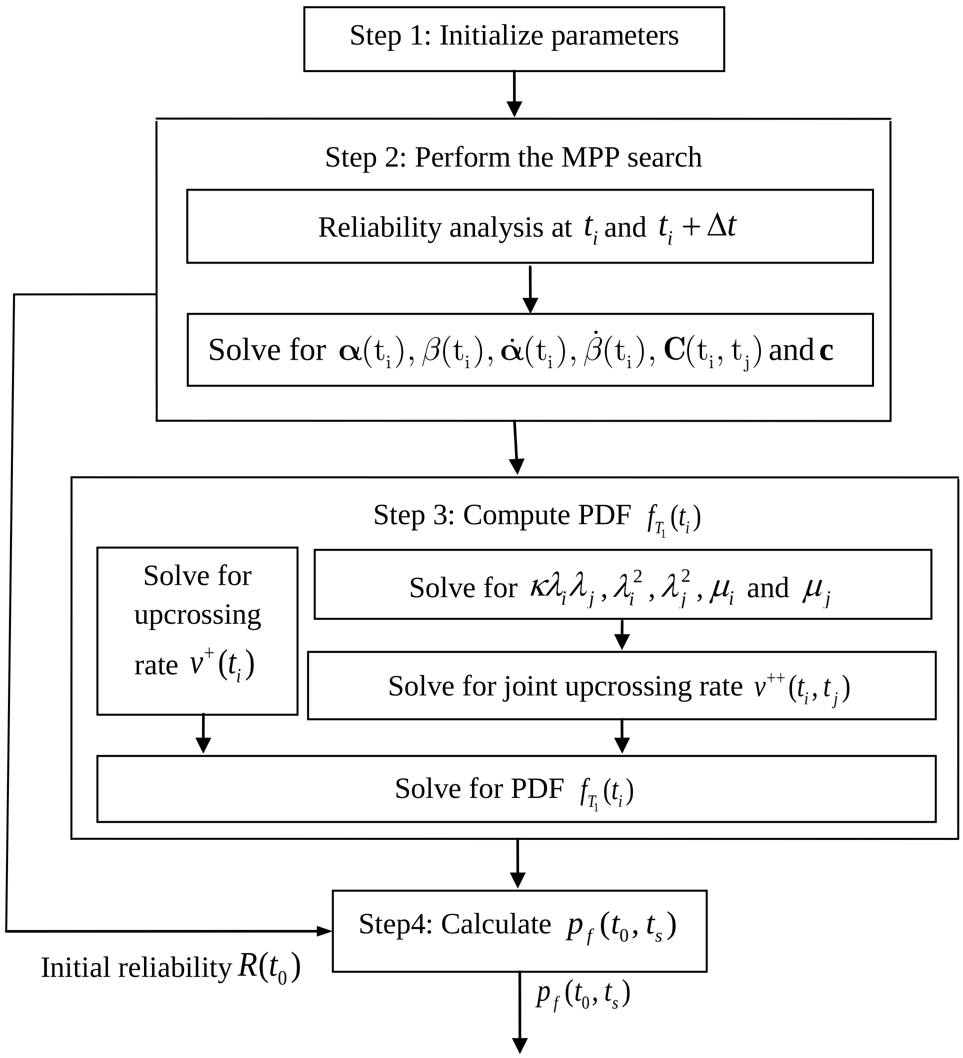

Figure1 Flowchart of the JUR/FORM

- Step 1: Initialize the random variables and stochastic processes, including transforming non-Gaussian variables into Gaussian ones, discretizing the time interval $[t_0, t_s]$ into $p+1$ time instants $t_0, t_1, \cdots, t_i, \cdots, t_{p+1} = t_s$, and setting a time step Δt for the MPP search at $t_i + \Delta t$ $(i = 1, 2, \cdots, p+1)$.

- Step 2: Perform the MPP search at every discretized point t_i, as well as at $t_i + \Delta t$; calculate $\boldsymbol{\alpha}(t_i)$, $\beta(t_i)$, $\dot{\boldsymbol{\alpha}}(t_i)$, $\dot{\beta}(t_i)$, covariance matrix $\mathbf{C}(t_i, t_j)$ $(i, j = 1, 2, \cdots, p+1)$, and $\mathbf{c}$ by using Eqs. (18), (35), (36) and (38)-(49).

- Step 3: Solve for the single upcrossing rate $v^{+}(t_i)$ using Eq. (15), joint upcrossing rate $v^{++}(t_i, t_j)$ $(i,\ j = 1, 2, \cdots,\ p+1)$ using Eq. (50), and compute the PDF $f_{T_1}(t_i)$ at each time instant using Eq. (14).
- Step 4: Calculate $p_f(t_0, t_s)$.

4. Numerical Examples

In this section, two examples are used to demonstrate the developed methodology. The first one is the reliability analysis of a corroded beam under time-variant random loading, and the second one is the reliability analysis of a two-slider crank mechanism. The two examples are selected because they represent two kinds of important applications. Specifically, the first example involves both of a stochastic process and random variables in the input of the limit-state function. The stochastic process is the time-variant random load acting on the beam. In the second example, there are no stochastic processes in the input of the limit-state function. But the limit-state function is still time-dependent because it is an explicit function of time.

To show the accuracy improvement of JUR/FORM, we compare its results with those of the traditional Poisson assumption based single upcrossing rate method, which has been reviewed in Sec II. Because the exact solutions are not available, we use Monte Carlo Simulation (MCS) as a benchmark.

In order to investigate the effects of parameter settings on the accuracy of JUR/FORM, numerical studies were also performed for Example 1. The effects studied include the effects of number of discretization points for the time interval $[t_0, t_s]$, the time step size Δt, the level of probability of failure, and the dependency of the limit-state function between two successive time instants.

Next we briefly review the MCS that we used.

4.1. Monte Carlo Simulation

When there are stochastic processes involved in the limit-state function, to generate the samples of the stochastic process Y_i, we treat the stochastic process as correlated random variables $\mathbf{Y}_i = (Y_i(t_1), Y_i(t_2), \cdots, Y_i(t_N))^T$ after discretizing the time interval $[t_0, t_s]$ into N instants. For a Gaussian stochastic process, the correlated random variables $\mathbf{Y}_i$ are generated after transforming the correlated random variables into uncorrelated ones as follows [47]

$$\mathbf{Y}_i = \boldsymbol{\mu}_{y_i} + \mathbf{L}\boldsymbol{\xi} \tag{54}$$

where $\boldsymbol{\xi} = (\xi_1, \xi_2, \cdots, \xi_N)^T$ is the vector of N independent standard normal random variables; $\boldsymbol{\mu}_{Y_i} = (\mu_{Y_i}(t_1), \mu_{Y_i}(t_2), \cdots, \mu_{Y_i}(t_N))^T$ are the vector of mean values of $\mathbf{Y}_i = (Y_i(t_1), Y_i(t_2), \cdots, Y_i(t_N))^T$; and $\mathbf{L}$ is a lower triangular matrix obtained from the covariance matrix of $\mathbf{Y}_i$.

Let matrix $\mathbf{A}_{N\times N}$ be the covariance matrix of $\mathbf{Y}_i$. $\mathbf{L}$ can be obtained by

$$\mathbf{A}_{N\times N} = \mathbf{PDP}^{-1} = \mathbf{LL}^T \tag{55}$$

in which $\mathbf{D}$ is a diagonal eigenvalue matrix of the covariance matrix $\mathbf{A}$, and $\mathbf{P}$ is the $N \times N$ square matrix whose i-th column is the i-th eigenvector of $\mathbf{A}$.

4.2. Example 1: Corroded beam under time-variant random loading

4.2.1 Problem statement

The beam problem in [45] is modified as our first example. As shown in Fig. 2, the cross section A-A of the beam is rectangular with its initial width a_0 and height b_0. Due to corrosion, the width and height of the beam decrease at a rate of r. A random load F acts at the midpoint of the beam. The beam is also subjected to a constant load due to the weight of the steel beam.

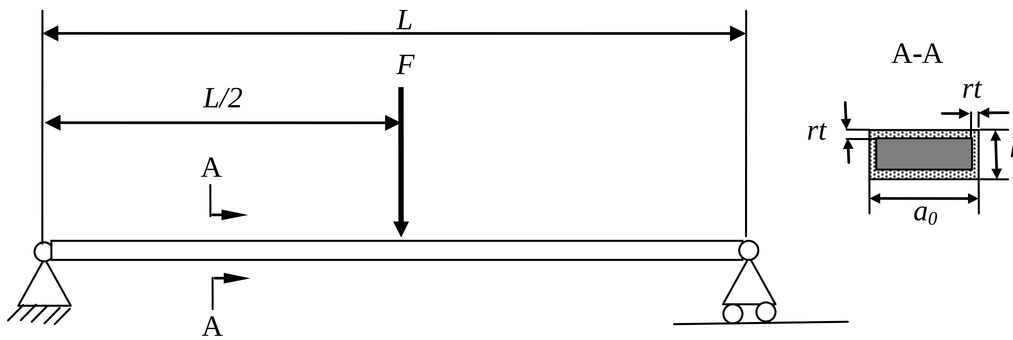

Figure 2 Corroded beam under time-variant random loading

A failure occurs as the stress of the beam exceeds the ultimate stress of the material, and the limit-state function is given by

$$g(\mathbf{X}, \mathbf{Y}, t) = \left(F(t)L/4 + \rho_{st} a_0 b_0 L^2 / 8\right) - \left(a_0 - 2rt\right)\left(b_0 - 2rt\right)\sigma_u / 4 \tag{56}$$

where σ_u is the ultimate strength, ρ_{st} is the density, and L is the length of the beam.

The variables and parameters in Eq. (56) are provided in Table 1.

Table 1 Variables and parameters of Example 1

Variable	Mean	Standard deviation	Distribution	Autocorrelation
a_0	0.2 m	0.01 m	Lognormal	N/A
b_0	0.04 m	4×10^{-3} m	Lognormal	N/A
σ_u	2.4×10^{8} Pa	2.4×10^{7} Pa	Lognormal	N/A
$F(t)$	3500 N	700 N	Gaussian	In Eq. (57)
L	5 m	0	Deterministic	N/A
ρ_{st}	78.5 kN/m^3	0	Deterministic	N/A
r	5×10^{-5} m/year	0	Deterministic	N/A

The auto-correlation function of the stochastic process $F(t)$ is given by

$$\rho^F(t_1, t_2) = \exp(-((t_2 - t_1)/\zeta)^2) \tag{57}$$

where $\zeta = 1$ year is the correlation length. The auto-correlation becomes weaker with a longer time interval $t_2 - t_1$.

4.2.2 Results

Following the numerical procedure of JUR/FORM in Fig.1, we computed the time-dependent probabilities of failure over different time intervals up to [0, 30] years. The time intervals were discretized into 80 small intervals, and the time size for the second MPP search was taken as 0.001 years. For MCS, the evaluated time intervals were discretized into 600 time instants with a sample size of 2×10^6 at each time instant to generate the stochastic loading $F(t)$. The results of the three methods are plotted in Fig. 3 and are given in Table 2. The relative errors, ε, with respect to the MCS solutions, and the confidence intervals (CI) of the MCS solutions, are also given in Table 2.

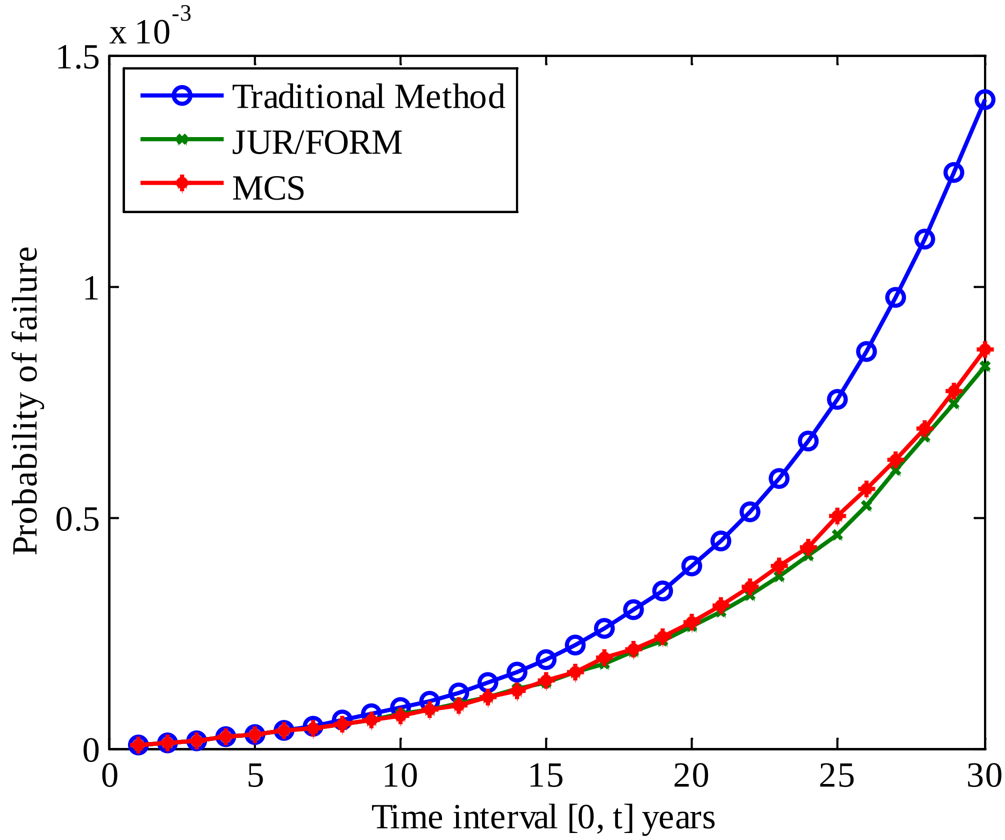

Figure 3 Probability of failure of the beam over different time intervals

Table 2 Time-dependent probabilities of failure

Time interval	Traditional Method		JUR/FORM		MCS	
	p_f	ε (%)	p_f	ε (%)	p_f	95% CI
[0, 5]	0.309×10^{-4}	6.55	0.292×10^{-4}	0.69	0.29×10^{-4}	$[0.215\times10^{-4}, 0.365\times10^{-4}]$
[0, 10]	0.864×10^{-4}	25.22	0.722×10^{-4}	4.64	0.69×10^{-4}	$[0.575\times10^{-4}, 0.805\times10^{-4}]$
[0, 15]	1.930×10^{-4}	31.29	1.435×10^{-4}	2.38	1.47×10^{-4}	$[1.302\times10^{-4}, 1.638\times10^{-4}]$
[0, 20]	3.924×10^{-4}	44.80	2.633×10^{-4}	2.84	2.71×10^{-4}	$[2.482\times10^{-4}, 2.938\times10^{-4}]$
[0, 25]	7.553×10^{-4}	50.76	4.625×10^{-4}	7.68	5.01×10^{-4}	$[4.700\times10^{-4}, 5.320\times10^{-4}]$
[0, 30]	14.027×10^{-4}	62.73	8.247×10^{-4}	4.33	8.62×10^{-4}	$[8.213\times10^{-4}, 9.027\times10^{-4}]$

The results indicate that the proposed JUR/FORM method is much more accurate than the traditional method. The traditional method leads to unacceptable errors while JUR/FORM shows excellent agreement with the MCS solution

In Table 3, we also give the numbers of function calls, N_{func}, as a measure of efficiency. The actual computational cost (times) is also given. The computational times were based on a Dell computer with Intel (R) Core (TM) i5-2400 CPU and 8GB system memory that we used. JUR/FORM produced much higher accuracy with a cost of increased computational effort, but the increased computational cost is moderate.

Table 3 Number of function calls and computational times

Time interval	Traditional Method		JUR/FORM		MCS	
	Time (s)	N_{func}	Cost (s)	N_{func}	Time (s)	N_{func}
[0, 5]	1.07	1250	6.19	5560	127.66	2×10^8
[0, 10]	1.04	1170	6.16	5280	1.29×10^3	4×10^8
[0, 15]	1.02	1155	6.27	5175	2.08×10^3	6×10^8
[0, 20]	1.03	1165	6.26	5195	2.70×10^3	8×10^8
[0, 25]	0.99	1135	6.23	5125	4.19×10^3	10×10^8
[0, 30]	2.61	2965	6.17	5005	4.51×10^3	12×10^8

4.2.3 Numerical studies

(a) Effect of discretization and time step size

As shown in the numerical procedure, the time interval $[t_0, t_s]$ is discretized into $p+1$ time instants t_i $(i = 0,1,2,\cdots, p)$ or p small intervals. The number of discretization points may affect the accuracy of the analysis result. If the number is too small, the error will be large. On the contrary, if the number is too large, the error will be small but the efficiency will be low.

To study the effect of the number of discretization points, we discretized the time interval [0, 30] years into 20, 30, 40, 50, 60, 70 and 80 small intervals.

Table 4 shows the results from JUR/FORM with different numbers of discretization points. When the time interval is divided into 20 small intervals, as expected, the error is the largest; however, the result is still more accurate than the traditional method. With the higher number of discretization points, the accuracy of JUR/FORM is higher.

Table 4 Time-dependent probability of failure with different discretization points

	MCS	Traditional Method	JUR/FORM with p small intervals						
			20	30	40	50	60	70	80
p_f (10^{-4})	8.6	14.027	7.83	7.98	8.09	8.13	8.21	8.24	8.25
ε (%)	N/A	62.73	9.16	7.42	6.15	5.68	4.76	4.41	4.33

In addition to the number of discretization, there is another parameter that may affect the performance of JUR/FORM. This parameter is the time-step size Δt, which is used for numerically evaluating the derivatives $\dot{\boldsymbol{\alpha}}(t_i)$ and $\dot{\beta}(t_i)$ in Eqs. (35) and (36), respectively. We used $\Delta t = 0.0005, 0.001, 0.005$ and 0.01 to study its effect. Table 5 provides the results, which show that the time-step size does affect the accuracy, but the effect is not significant. The general discussions regarding the effect of a step size for numerical derivatives can be also found in [48-50].

Table 5 Time-dependent probability of failure with different Δt

Method	MCS	Traditional Method	JUR/FORM with different Δt			
			5×10^{-4}	0.001	0.005	0.01
p_f(10^{-4})	8.62	14.03	8.41	8.25	8.0	7.98
ε (%)	N/A	62.73	2.47	4.33	7.16	7.40

(b) Effect of larger probability of failure

To investigate the accuracy of JUR/FORM when the probability of failure becomes larger, we compared the results of MCS, JUR/FORM and traditional method for six cases at different probability levels. Table 6 show that the larger is the probability of failure, the worse is the traditional method, while JUR/FORM is always much more accurate than the traditional method.

Table 6 Time-dependent probability of failure UR/FORM at different probability levels

Traditional Method		JUR/FORM		MCS	
p_f	ε (%)	p_f	ε (%)	p_f	95% CI
14×10^{-4}	71.15	8.25×10^{-4}	0.86	8.18×10^{-4}	$[7.62\times10^{-4}, 8.74\times10^{-4}]$
19×10^{-4}	72.73	10×10^{-4}	9.09	11×10^{-4}	$[10.4\times10^{-4}, 11.6\times10^{-4}]$
95×10^{-4}	93.88	46×10^{-4}	6.12	49×10^{-4}	$[47.6\times10^{-4}, 50.4\times10^{-4}]$
176×10^{-4}	97.75	83×10^{-4}	6.74	89×10^{-4}	$[87.2\times10^{-4}, 90.8\times10^{-4}]$
1083×10^{-4}	127.52	444×10^{-4}	6.72	476×10^{-4}	$[472\times10^{-4}, 480\times10^{-4}]$
3101×10^{-4}	137.81	1246×10^{-4}	4.44	1304×10^{-4}	$[1297\times10^{-4}, 1311\times10^{-4}]$

(c) Effect of the auto-covariance of the limit-state function

JUR/FORM is developed to better account for dependent failures over a time period. To demonstrate this, we analyzed the accuracy of JUR/FORM for five cases with different levels of dependency. Fig. 4 shows for the five cases the coefficients of auto-correlation ρ, ranging from 0.108 to 0.961, between two successive time instants $[t_i, t_{i+1}]$, $i = 1, 2, \cdots, 99$ over [0, 30] years. Note that the coefficient of auto-correlation of the limit-state function is almost constant given the auto-correlation function of the stochastic process for the external force in Eq. (57).

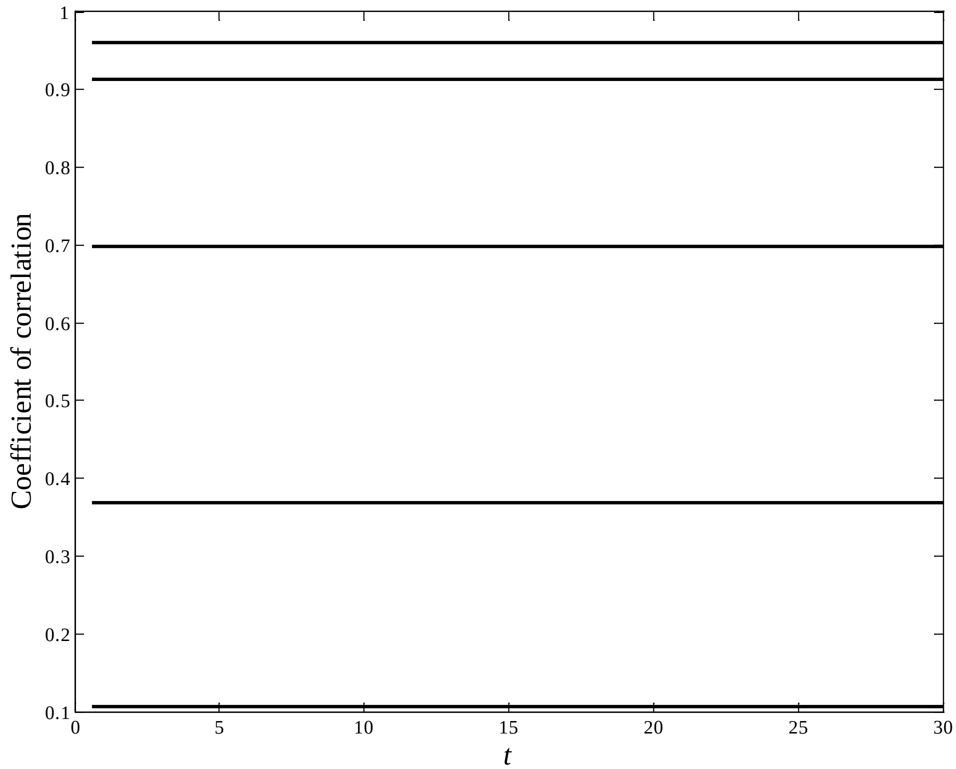

Figure 4 Coefficient of correlation between two successive time instants

Table 7 shows that the error of the traditional method decreases when the dependency becomes weaker while the accuracy of JUR/FORM method is always better than the traditional effort.

Table 7 Time-dependent probability of failure with different dependencies

ρ	Traditional Method		JUR/FORM		MCS	
	p_f (10^{-4})	ε (%)	p_f (10^{-4})	ε (%)	p_f(10^{-4})	95% CI (10^{-4})
0.961	4.756	24.5	5.83	7.46	6.30	[5.81, 6.79]
0.914	6.952	23.18	8.52	5.86	9.05	[8.46, 9.64]

0.698	13.54	20.07	16.60	2.01	16.94	[16.13, 17.75]
0.368	22.32	17.27	27.36	1.41	26.98	[25.96, 28.00]
0.108	33.29	12.12	38.65	2.03	37.88	[36.68, 39.08]

4.3. Example 2: Two-slider crank mechanism

A two-slider crank mechanism is shown in Fig. 5. This type of mechanism is widely used in engines. The crank is rotating at an angular velocity of ω. The motion error is defined as the difference between the desired displacement difference and the actual displacement difference between sliders *A* and *B*. The error should not exceed 0.94 mm over one motion cycle.

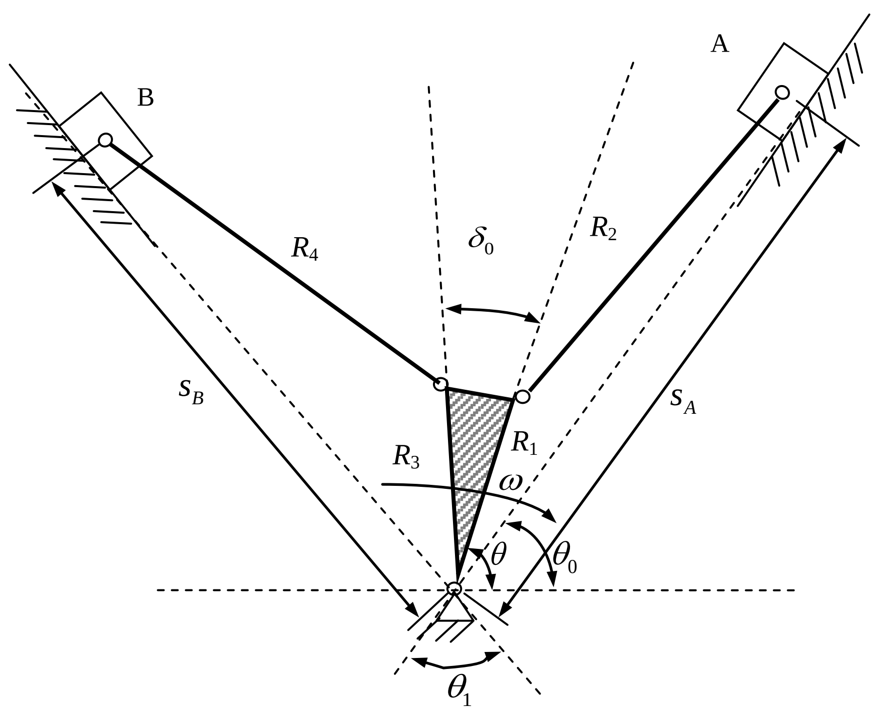

Figure 5. Two-slider crank mechanism

The limit-state function is given by

$$g(\mathbf{X}, \mathbf{Y}, t) = \Delta s_{desired} - \Delta s_{actual} \tag{58}$$

in which

$$\begin{aligned}\Delta s_{actual} &= R_1 \cos(\theta - \theta_0) + \sqrt{R_2^2 - R_1^2 \sin^2(\theta - \theta_0)} \\ &- R_3 \cos(\theta_1 + \theta_0 - \theta - \delta_0) - \sqrt{R_4^2 - R_3^2 \sin^2(\theta_1 + \theta_0 - \theta - \delta_0)}\end{aligned} \tag{59}$$

$$\begin{aligned}\Delta s_{desired} &= 108 \cos(\theta - \theta_0) + \sqrt{211^2 - 108^2 \sin^2(\theta - \theta_0)} \\ &- 100 \cos(\theta_1 + \theta_0 - \theta - \delta_0) - \sqrt{213^2 - 100^2 \sin^2(\theta_1 + \theta_0 - \theta - \delta_0)}\end{aligned} \tag{60}$$

The variables and parameters in the limit-state function are given in Table 8.

Table 8 Variables and parameters in Example 2

Variable	Mean	Standard deviation	Distribution
R_1	108 mm	0.05 mm	Normal
R_2	211 mm	0.2 mm	Normal
R_3	100 mm	0.05 mm	Normal
R_4	213 mm	0.2 mm	Normal
θ_0	45°	0	Deterministic
θ_1	60°	0	Deterministic
δ_0	10°	0	Deterministic
ω	π rad/s	0	Deterministic

This mechanism problem is different from the beam problem in the follow two aspects. First, this problem does not involve any input stochastic processes, but the limit-state function is still a stochastic process because it is a function of time. Second, the dependence of the limit-state function at any two time instants is strong. The auto-dependence does not decay with a longer time period. On the contrary, in the first problem, the auto-dependency between the performance values at t_1 and t_2 will be weaker and weaker when $t_2 - t_1$ becomes larger and larger as indicated in Eq. (57).

The angular velocity of the crank is $\omega = \pi$ rad/s, and the time period of one motion cycle is then [0, 2] seconds**.** Following the numerical procedure of JUR/FORM, we computed the probabilities of failure over different time intervals. Each of the evaluated time intervals were discretized into 60 smaller intervals. The step size for the second MPP search was 8×10^{-5} seconds. The traditional method and MCS with a sample size of 10^6 were also applied. The results from the three methods are plotted in Fig. 6 and are given in Table 9.

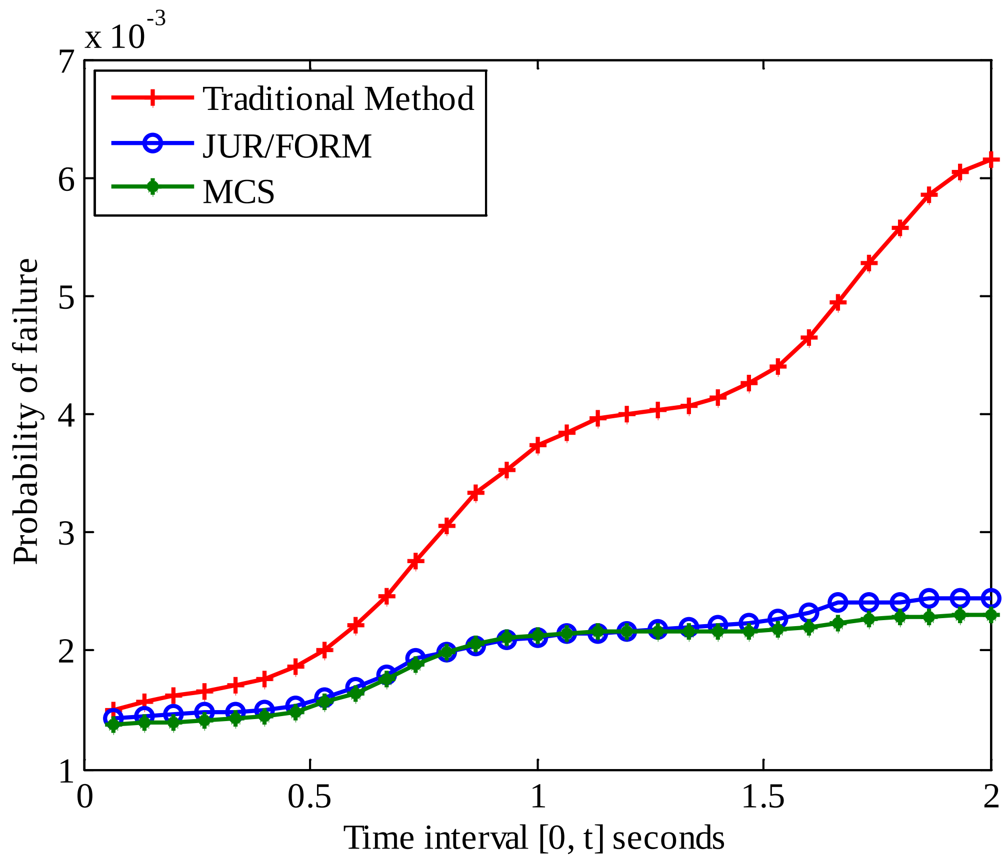

Figure 6 Time-dependent probabilities of failure

Table 9 Time-dependent probabilities of failure

Time interval	Traditional Method		JUR/FORM		MCS	
	p_f (10^{-3})	ε (%)	p_f (10^{-3})	ε (%)	p_f (10^{-3})	95% CI (10^{-3})
[0, 0.4]	1.76	22.03	1.51	4.27	1.45	[1.37, 1.52]
[0, 0.8]	3.06	53.84	1.99	0.08	1.99	[1.90, 2.08]
[0, 1.2]	4.01	85.72	2.16	0.17	2.16	[2.07^{3}, 2.25]
[0, 1.6]	4.64	111.46	2.32	5.40	2.20	[2.10, 2.29]
[0, 2.0]	6.16	168.36	2.44	6.27	2.30	[2.20, 2.39]

Table 10 Number of function calls and MPP searches

Time interval	Traditional Method		JUR/FORM		MCS	
	MPP searches	Function Calls	MPP searches	Function Calls	MPP searches	Function Calls
[0, 0.4]	216	1927	120	2452	N/A	6×10^{7}
[0, 0.8]	96	720	120	2455	N/A	1.2×10^{8}
[0, 1.2]	96	4320	120	2437	N/A	1.8×10^{8}
[0, 1.6]	156	3140	120	2451	N/A	2.4×10^{8}
[0, 2.0]	816	16531	120	2437	N/A	3.0×10^{8}

The results indicate that JUR/FORM is significantly more accurate than the traditional method. The number of MPP searches and function calls are provided in Table 10. The increased computational cost by JUR/FORM is reasonable given its significantly improved accuracy. From Table 10, we also see that JUR/FORM does not always require more function calls than the traditional method as in the cases for the time periods [0, 1.2], [0, 1.6] and [0, 2.0]. The reason is that the traditional method needs to numerically solve the integral in Eq. (6). For a shorter time period, the numerical integration may need more function calls than JUR/FORM where the number of discretization points may not need to be high for short time periods.

5. Conclusion

Time-dependent reliability analysis is needed in many engineering applications. When multiple dependent upcrossings occur over a time interval, the single upcrossing rate method with Poisson assumption may produce large errors in estimating the time-dependent probability of failure.

This work demonstrates that the joint upcrossing rates proposed in [44] can be extended to a general time-dependent limit-state function with much higher accuracy. This work integrates the FORM with the joint upcrossing rates so that high computational efficiency can be maintained. Analytical expressions of the single and joint upcrossing rates are also derived based on FORM.

The proposed method has shown good accuracy when the probability of failure is small and the dependency between failures is strong. When the probability of failure becomes larger or the dependency becomes weaker, the proposed method remains more accurate than the traditional upcrossing rate method. Since the proposed method requires a numerical method in solving the integral equation and derivatives, its accuracy may be affected by the number of discretization points and the time size between two consecutive MPP searches.

Possible future work includes improving the efficiency and robustness of the method and applying it to time-dependent reliability-based design optimization.

Acknowledgement

The authors gratefully acknowledge the support from the Office of Naval Research through contract ONR N000141010923 (Program Manager – Dr. Michele Anderson) and the National Science Foundation through grant CMMI 1234855.

Reference

[1] S.K. Choi, R.V. Grandhi, R.A. Canfield, Reliability-based structural design, Springer, 2007.

[2] X. Du, A. Sudjianto, B. Huang, Reliability-based design with the mixture of random and interval variables, Journal of Mechanical Design, Transactions of the ASME, 127 (2005) 1068-1076.

[3] B. Huang, X. Du, Probabilistic uncertainty analysis by mean-value first order Saddlepoint Approximation, Reliability Engineering and System Safety, 93 (2008) 325-336.

[4] J. Zhang, X. Du, A second-order reliability method with first-order efficiency, Journal of Mechanical Design, Transactions of the ASME, 132 (2010).

[5] H.O. Madsen, Krenk, S., Lind, N.C., Methods of Structural Safety, Englewood Cliffs, New Jersey, 1986.

[6] B. Banerjee, B.G. Smith, Reliability analysis for inserts in sandwich composites, Advanced Materials Research, 275 (2011) pp. 234-238.

[7] D.W. Kim, S.S. Jung, Y.H. Sung, D.H. Kim, Optimization of SMES windings utilizing the first-order reliability method, Transactions of the Korean Institute of Electrical Engineers, 60 (2011) 1354-1359.

[8] H. Millwater, Y. Feng, Probabilistic sensitivity analysis with respect to bounds of truncated distributions, Journal of Mechanical Design, Transactions of the ASME, 133 (2011).

[9] R.A. Miller, Thermal barrier coatings for aircraft engines: History and directions, Journal of Thermal Spray Technology, 6 (1997) 35-42.

[10] S. Dubowsky, M. Norris, E. Aloni, A. Tamir, Analytical and experimental study of the prediction of impacts in planar mechanical system with clearance, Journal of mechanisms, transmissions, and automation in design, 106 (1984) 444-451.

[11] M. Dupac, D.G. Beale, Dynamic analysis of a flexible linkage mechanism with cracks and clearance, Mechanism and Machine Theory, 45 (2010) 1909-1923.

[12] M.J. Tsai, T.H. Lai, Accuracy analysis of a multi-loop linkage with joint clearances, Mechanism and Machine Theory, 43 (2008) 1141-1157.

[13] J. Meng, Z. Li, A general approach for accuracy analysis of parallel manipulators with joint clearance, in IEEE/RSJ International Conference on Intelligent Robots and Systems, 2005, pp. 790-795.

[14] T. Szkodny, The sensitivities of industrial robot manipulators to errors of motion models' parameters, Mechanism and Machine Theory, 36 (2001) 673-682.

[15] U.D. Nielsen, Calculation of mean outcrossing rates of non-Gaussian processes with stochastic input parameters - Reliability of containers stowed on ships in severe sea, Probabilistic Engineering Mechanics, 25 (2010) 206-217.

[16] N. Kuschel, R. Rackwitz, Optimal design under time-variant reliability constraints, Structural Safety, 22 (2000) 113-127.

[17] O. Ditlevsen, Stochastic model for joint wave and wind loads on offshore structures, Structural Safety, 24 (2002) 139-163.

[18] J.R. Rice, Beer, F.P.,, First-Occurrence Time of Hih-Level Crossings in a Continuous Random Process, The Journal of Acoustical Society of America, 39 (1965) 323-335.

[19] V.F. Richard, Mircea, D.G., Reliability of Dynamic Systems Under Limited Information, in: SAND2006-5580 (Ed.) Sandia report, 2006.

[20] J. Song, A. Der Kiureghian, Joint first-passage probability and reliability of systems under stochastic excitation, Journal of Engineering Mechanics, 132 (2006) 65-77.

[21] J.B. Chen, J. Li, The inherent correlation of the structural response and reliability evaluation, Jisuan Lixue Xuebao/Chinese Journal of Computational Mechanics, 25 (2008) 521-528.

[22] J. Li, J.b. Chen, W.l. Fan, The equivalent extreme-value event and evaluation of the structural system reliability, Structural Safety, 29 (2007) 112-131.

[23] J.B. Chen, J. Li, The extreme value distribution and dynamic reliability analysis of nonlinear structures with uncertain parameters, Structural Safety, 29 (2007) 77-93.

[24] S.O. Rice, Mathematical Analysis of Random Noise, Bell System Technical Journal, 23 (1944) 282–332.

[25] V. Rui, The Theory of Statistics of Extremes and EL NINO Phenomena-A Stochastic Approach. Massachusetts Institute of Technology, Boston, 1985.

[26] G. Schall, M.H. Faber, R. Rackwitz, Ergodicity assumption for sea states in the reliability estimation of offshore structures, Journal of Offshore Mechanics and Arctic Engineering, 113 (1991) 241-246.

[27] S. Engelund, R. Rackwitz, C. Lange, Approximations of first-passage times for differentiable processes based on higher-order threshold crossings, Probabilistic Engineering Mechanics, 10 (1995) 53-60.

[28] R. Rackwitz, Computational techniques in stationary and non-stationary load combination - A review and some extensions, Journal of Structural Engineering (Madras), 25 (1998) 1-20.

[29] L.D. Lutes, and Sarkani, S., , Random Vibrations: Analysis of Structural and Mechanical Systems, Elsevier, New York., 2004.

[30] L.D. Lutes, and Sarkani, S., , Reliability Analysis of Systems Subject to First-Passage Failure, in: NASA Technical Report No. NASA/CR-2009-215782, 2009.

[31] B. Sudret, Analytical derivation of the outcrossing rate in time-variant reliability problems, Structure and Infrastructure Engineering, 4 (2008) 353-362.

[32] J. Zhang, X. Du, Time-dependent reliability analysis for function generator mechanisms, Journal of Mechanical Design, Transactions of the ASME, 133 (2011).

[33] Y.K. Lin, Probabilistic Theory of Structural Dynamics., McGraw-HilI, New York, 1967.

[34] H. Cramer, On the intersections between the trajectories of a normal stationary stochastic process and a high level, Arkiv för Matematik 6(1966) 337-349.

[35] O. Hagen, Conditional and joint failure surface crossing of stochastic processes, Journal of Engineering Mechanics, 118 (1992) 1814-1839.

[36] C.W. Li, R.E. Melchers, Structural systems reliability under stochastic loads, Proceedings of the Institution of Civil Engineers: Structures and Buildings, 104 (1994) 251-256.

[37] D.B. Parkinson, Second order stochastic simulation with specified correlation, Advances in engineering software, 30 (1999) 489-494.

[38] H. Streicher, R. Rackwitz, Time-variant reliability-oriented structural optimization and a renewal model for life-cycle costing, Probabilistic Engineering Mechanics, 19 (2004) 171-183.

[39] J.N. Yang, M. Shinozuka, On the first excursion probability in stationary narrow- band random vibration, Journal of Applied Mechanics, Transactions ASME, 38 Ser E (1971) 1017-1022.

[40] J.N. Yang, M. Shinozuka, On the first-excursion probability in stationary narrow-band random vibration - 2, Journal of Applied Mechanics, Transactions ASME, 39 Ser E (1972) 733-738.

[41] E.H. Vanmarcke, On the distribution of the first-passage time for normal stationary random processes, Journal of Applied Mechanics, Transactions ASME, 42 Ser E (1975) 215-220.

[42] A. Preumont, On the peak factor of stationary Gaussian processes, Journal of Sound and Vibration, 100 (1985) 15-34.

[43] M.C. Bernard, J.W. Shipley, The first passage problem for stationary random structural vibration, Journal of Sound and Vibration, 24 (1972) 121-132.

[44] P.H. Madsen, S. Krenk, Integral equation method for the first-passage problem in random vibration, Journal of Applied Mechanics, Transactions ASME, 51 (1984) 674-679.

[45] C. Andrieu-Renaud, B. Sudret, M. Lemaire, The PHI2 method: A way to compute time-variant reliability, Reliability Engineering and System Safety, 84 (2004) 75-86.

[46] S.O. Rice, Mathematical analysis of random noise, Bell Syst.Tech. J., 24 (1945) 146-156.

[47] A.K. Gupta, T.F. Móri, G.J. Székely, How to transform correlated random variables into uncorrelated ones, Applied Mathematics Letters, 13 (2000) 31-33.

[48] V. Aristov, A. Stroganov, A method of formalizing computer operations for solving nonlinear differential equations, Applied Mathematics and Computation, 218 (2012) 8083-8098.

[49] S. Kamal, Stabilization of stochastic approximation by step size adaptation, Systems and Control Letters, 61 (2012) 543-548.

[50] L. Wang, R.V. Grandhi, D.A. Hopkins, Structural reliability optimization using an efficient safety index calculation procedure, International Journal for Numerical Methods in Engineering, 38 (1995) 1721-1738.